IEEE Access
Multidisciplinary | Rapid Review | Open Access Journal

Received April 1, 2019, accepted April 27, 2019, date of publication May 8, 2019, date of current version May 20, 2019.

Digital Object Identifier 10.1109/ACCESS.2019.2915612

Denoising and Baseline Drift Removal Method of MEMS Hydrophone Signal Based on VMD and Wavelet Threshold Processing

HONGPING HU[1], LINMEI ZHANG[1], HUICHAO YAN[1,2], YANPING BAI[1], AND PENG WANG[1]
[1]Department of Mathematics, School of Science, North University of China, Taiyuan 030051, China
[2]School of Information and Communication Engineering, North University of China, Taiyuan 030051, China

Corresponding author: Hongping Hu (hhp92@163.com)

This work was supported in part by the Shanxi Natural Science Foundation under Grant 201801D121026, Grant 201701D121012, and Grant 201701D221121, in part by the National Nature Science Foundation of China under Grant 61774137, and in part by the Shanxi Scholarship Council of China under Grant 2016-088.

ABSTRACT Aiming at the problem that the signals received by MEMS vector hydrophones are mixed with a large amount of external environmental noise, and inevitably produce baseline drift and other distortion phenomenons which made it difficult for the further signal detection and recognition, a joint denoising method (VMD-NWT) based on variational mode decomposition (VMD) and nonlinear wavelet threshold (NWT) processing is proposed. The main frequency of the noisy signal is first obtained by Fourier transform. Then the noisy signal is decomposed by VMD to obtain the IMF components. The center frequency and correlation coefficient of each IMF component further determine that the IMF components belong to noise IMF components, noisy IMF components or pure IMF components. Then the pure IMF components are reserved, the noise IMF components are removed, and the noisy IMF components are denoised by NWT processing method with new threshold function as a whole. Finally, the denoised IMF components and the pure IMF components are reconstructed to obtain the denoised signal to realize the extraction of useful signals and baseline drift removal. Compared with complete ensemble empirical mode decomposition with adaptive noise combined with wavelet threshold processing method (CEEMDAN-WT), ensemble empirical mode decomposition combined with wavelet threshold processing method (EEMD-WT), and single wavelet threshold processing method with compromised function between hard and soft threshold (ZWT), the VMD-NWT in this paper has the advantages of less calculation and simple implementation. The simulation comparison experiments verify that the VMD-NWT is superior to CEEMDAN-WT, EEMD-WT, and ZWT. Then VMD-NWT is applied to process the measured data obtained from the Fenji experiment conducted by the North University of China. Simulation and lake trial results show that VMD-NWT has better denoising effect and can realize baseline drift removal. So the proposed VMD-NWT has certain practical research value.

INDEX TERMS Baseline drift, MEMS hydrophone, signal denoising, variational mode decomposition (VMD), nonlinear wavelet threshold (NWT) processing.

I. INTRODUCTION

The MEMS vector hydrophone which imitates the line sensing system of fish has been used to realize underwater acoustic signal detection by extracting the change of resistance through the detection system. With excellent performance [1]–[3], it could be widely applied to explore the position, state parameters, types and other information of certain targets in the ocean, lakes and other underwater acoustic environment. However, the noise in the acoustic environment is complex and changeable. The various sound source including natural sources such as wave, marine life and rain, unnatural sources such as ships and military sonar [4], et al. will lead to the results that the collected target signals are mixed with a lot of noise and inevitably produce baseline drift and other distortion phenomenons. The further

The associate editor coordinating the review of this manuscript and approving it for publication was Liangtian Wan.

signal detection, recognition, feature extraction and classification require that the raw signal waveforms have less noise and distortion. Therefore, denoising the noisy signal and correcting the baseline drift are greatly significant for the further signal detection and recognition.

Many methods have been used to denoise the noisy and correct baseline drift in various signals. The traditional signal denoising methods are based on finite impulse response (FIR) [5] and infinite impulse response (IIR)[6]. The noise could be denoised by using the conventional frequency domain filtering methods if the signal and noise have separate bandwidth. However, these denoising methods do not always perform well when applied to non-stationary signals and have little effect in correcting signal drift. L.Pablo et al. used an adaptive filter to remove the baseline wander of ECGs [7]. However, this algorithm is time consuming and had some problems on convergence. Moreover, it was always not realistic for adaptive filter to obtain a suitable reference signal. Based on a set of predefined basis functions, wavelet transform method is used to make signal denoised by decomposing the measured signals followed by suppression of components corresponding to noise [8]. The universal hard thresholding wavelet shrinkage method applied a hard-thresholding function to the wavelet coefficients when considering the universal threshold [9]. The improved wavelet thresholding method used thresholding function based on the sigmoid function when considering the universal threshold [10]. Because the wavelet ′s frequency resolution was higher at low frequencies than that at high frequencies, literature [11] made use of its frequency resolution in low frequencies to estimate the baseline drift and then removed it from the noisy pulse signal. Empirical Mode Decomposition (EMD) [12] had been proposed by Huang et al. to denoise the noise contained in signals. Unlike these wavelet-based methods, EMD had the obvious advantage of not relying on the predefined basis functions and other parameters. Intrinsic Mode Functions (IMFs) are separated adaptively from the data set. However, this method is prone to mode mixing, especially when the noise was present intermittently. The mode mixing refers to the existence of different time scales in a single IMF or the same time scale in different IMFs. The problem of mode mixing in EMD was solved preferably by a modified noise assisted data analysis method known as Ensemble Empirical Mode Decomposition method namely EEMD [13]. In the EEMD method, the amplitude of noise which was added to the observed signal to prevent the mode mixing effect played an important role especially in view of the requirement to preserve the signal integrity during its reconstruction. The EEMD analysis reported in [14] was applied to denoise the physiological signals such as ECG, which is based on the reconstruction of the signal using a partial sum of selected IMFs. The ECG ′s denoising used by EEMD reported in [15] also realized the partial reconstruction of the IMFs based on the empirical energy model of IMFs, which required that the first IMF should always be the noise-only IMF. However, in practice, it was not always valid to have the first IMF to be a noise-only IMF. In [16], Mariyappa *et al.* proposed a method which involved filtering the first order IMF by interval thresholding, adding the rest of the IMFs passing through the interval thresholded window followed by the reconstruction of the target signal, and eliminating the baseline drift contained in the noisy signal adopted the EEMD method. But it should be noticed that the noise amplitudes employed in the EEMD method to prevent mode mixing should be neither too small nor too large. And the inappropriate noise amplitudes might fail to achieve the prevention of mode mixing. Also, the another problem which existed in EEMD was that this algorithm took more time to produce output due to more number of iterations and also the produced output signal needed to be improved [4].

Variational Mode Decomposition (VMD) [17] proposed by Dragomiretskiy in 2013 was an adaptive and non-recursive signal decomposition method, which could realize the signal segmentation in frequency domain and the components separation effectively. Compared to EEMD, VMD which has strong mathematical foundation could achieve accurate signal separation at the same time and had better noise robustness and higher computational efficiency. With the excellent effect on signal-noise separation, VMD algorithm has been used in many fields after it was proposed. For example, a multi-objective particle swarm optimization (MOPSO) algorithm is proposed to optimize the parameters of VMD, and then it is applied to the composite fault diagnosis of the gearbox and can successfully extracts the composite fault characteristics of the gearbox under a strong background noise environment in [18]; A feature recognition and fault diagnosis method was proposed based on VMD and deep neural networks (DNN) in [19], which could effectively extract sensitive feature and recognize vibration of faults state; A intraday stock price hybrid predictive model was proposed based on variational mode decomposition model and back propagation neural network in [20], which was superior to the baseline predictive model.

Aiming at the problem on strong noise interference and baseline drift in the data acquisition of MEMS vector hydrophone, this paper proposes a new joint denoising method based on VMD and nonlinear wavelet threshold (NWT) processing, VMD-NWT. In this paper, VMD-NWT method is used to make the simulated signal and the Fenji lake trial data obtained from North University of China denoised. Compared with the similar algorithms, the principle of the proposed algorithm is simpler and has less computational complexity. And its effect on denoising and correcting baseline drift of hydrophone signals are better than the contrast algorithms.

The outline of this paper is as follows. Section 1 is the introduction. The VMD algorithm and nonlinear wavelet threshold processing are reviewed briefly in Section 2.1 and Section 2.2, and the proposed method VMD-NWT are described in detail in Section 3. Experimental results and analysis for denosing are given in Section 4 for the simulated

signal and the Fenji lake trial data obtained from North University of China. Section 5 is the conclusion.

II. BASIC PRINCIPLE

A. VARIATIONAL MODE DECOMPOSITION

The purpose of Variational Mode Decomposition (VMD) is to decompose the input real valued signal into an ensemble of Intrinsic Mode Functions (IMFs) which have limited bandwidth and online estimated center frequencies [19]. And the bandwidth is estimated as the following steps:

Step 1: For each mode, obtaining its unilateral spectrum by computing the associated analytic signal through the Hilbert transform, $(\delta(t) + \frac{i}{\pi t}) * u_k(t)$, where $\delta(t)$ is the Dirichlet function, $i^2 = -1$ and $*$ is the convolution symbol.

Step 2: For each mode, modulating its frequency spectrum to the corresponding 'baseband', by multiplying an exponential modulated signal $e^{-i\omega_k(t)}$ that has the pre-estimated center frequency, $[(\delta(t) + \frac{i}{\pi t}) * u_k(t)]e^{-i\omega_k(t)}$.

Step 3: The bandwidth is estimated through the squared-norm of the modulated signal's gradient. The constrained variational problem is obtained as follows:

$$\begin{cases} \min\limits_{\{u_k\},\{\omega_k\}} \{\sum_k \|\partial_t[(\delta(t) + \dfrac{i}{\pi t}) * u_k(t)]e^{-i\omega_k(t)}\|_2^2\} \\ s.t. \sum_k u_k = f. \end{cases} \tag{1}$$

where $\{u_k\} = \{u_1, u_2, ..., u_K\}$ and $\{\omega_k\} = \{\omega_1, \omega_2, ..., \omega_K\}$ are the set of all modes and the corresponding center frequencies, respectively.

In order to solve the optimal solution of the above variational problem (1), problem (1) is transformed into an unconstrained variational problem through introducing the Lagrange multiplication operator. And the augmented Lagrange L is as follows:

$$\begin{aligned} &L(\{u_k\}, \{\omega_k\}, \lambda) \\ &= \alpha\{\sum_k \|\partial_t[(\delta(t) + \frac{i}{\pi t}) * u_k(t)]e^{-i\omega_k(t)}\|_2^2\} \\ &\quad + \|f(t) - \sum_k u_k(t)\|_2^2 + \langle\lambda(t), f(t) - \sum_k u_k(t)\rangle. \end{aligned} \tag{2}$$

where α denotes the balancing parameter of the data-fidelity constraint. Equation (2) is then solved with the alternate direction method of multipliers (ADMM). The optimal is directly updated by Wiener filtering in Fourier domain. Thus Wiener filtering is embedded in the VMD, which makes sampling and noise more robust. The mode in Fourier domain is obtained as follows:

$$\hat{u_k}^{n+1}(\omega) = \frac{\hat{f}(\omega) - \sum_{l\neq k} \hat{u}_l(\omega) + \frac{\hat{\lambda}(\omega)}{2}}{1 + 2\alpha(\omega - \omega_k)^2}. \tag{3}$$

where ω is frequency, $\hat{u}_k^{n+1}(\omega), \hat{f}(\omega), \hat{\lambda}(\omega)$ are the corresponding Fourier transform of $u_k^{n+1}(t), f(t), \lambda(t)$,and n means the *nth* loop iteration. In the algorithm, the center frequencies is re-estimated according to the center of gravity of the corresponding mode ' s power spectrum. The iterative formula of ω_k^{n+1} is as follows:

$$\omega_k^{n+1} = \frac{\int_0^\infty \omega|\hat{u}_k^{n+1}(\omega)|^2 d\omega}{\int_0^\infty |\hat{u}_k^{n+1}(\omega)|^2 d\omega}. \tag{4}$$

The Lagrangian multipliers λ is updated according to (5):

$$\hat{\lambda}^{n+1}(\omega) = \hat{\lambda}^n(\omega) + \tau[\hat{f}(\omega) - \sum_k \hat{u}_k^{n+1}(\omega)]. \tag{5}$$

where τ is the step size of the dual ascent, and setting τ to 0 can effectively turn off the lagrangian multiplier to ensure that the algorithm converges effectively.

The iteration and loop to solve the problem (1) is stopped until the equation $\sum_k \frac{\|u_k^{n+1} - u_k^n\|_2^2}{\|u_k^n\|_2^2} < \varepsilon$ is satisfied, where ε is convergence tolerance.

B. NONLINEAR WAVELET THRESHOLDING METHOD

The nonlinear wavelet threshold (NWT) method is applicable for processing signals with white noise. Wavelet transform can concentrate the signal energy on a few wavelet coefficients and the transformation of white noise on any basis function is still white noise with the same amplitude. Relatively, the wavelet coefficient values of the useful signal are bound to be greater than those of the white noise with scattered energy and small amplitude [21]. Appropriate threshold value and threshold function are selected, and then the wavelet coefficients of the noisy signal is processed by thresholding method. Thus the goal of removing noise and retaining useful signal is achieved. At present, the hard and soft threshold denoising method proposed by Dohono [22] is most widely used in engineering, defined as (6)-(7) :

$$\hat{\omega}_{j,k} = \begin{cases} \omega_{j,k}, & |\omega_{j,k}| \geq thr \\ 0, & |\omega_{j,k}| < thr. \end{cases} \tag{6}$$

$$\hat{\omega}_{j,k} = \begin{cases} sgn(\omega_{j,k})(|\omega_{j,k}| - thr), & |\omega_{j,k}| \geq thr \\ 0, & |\omega_{j,k}| < thr. \end{cases} \tag{7}$$

where $\omega_{j,k}$ is the wavelet transform coefficients of the noisy observation signal, $sgn()$ is the symbolic function, thr is the threshold, and $\hat{w}_{j,k}$ is the estimated coefficients of the real signal.

However, the hard threshold function is discontinuous at the point of threshold, which causes the estimated signal to generate additional oscillations. The soft threshold function avoids additional oscillations, but there is a constant deviation between the estimated value and true value. Thus many scholars have tried to propose improved threshold functions to improve the denoising effect of wavelet threshold method. In [23], the compromised method between soft and hard threshold is proposed, defined as (8) .

$$\hat{\omega}_{j,k} = \begin{cases} sgn(\omega_{j,k})(|\omega_{j,k}| - \beta \cdot thr), & |\omega_{j,k}| \geq thr \\ 0, & |\omega_{j,k}| < thr. \end{cases} \tag{8}$$

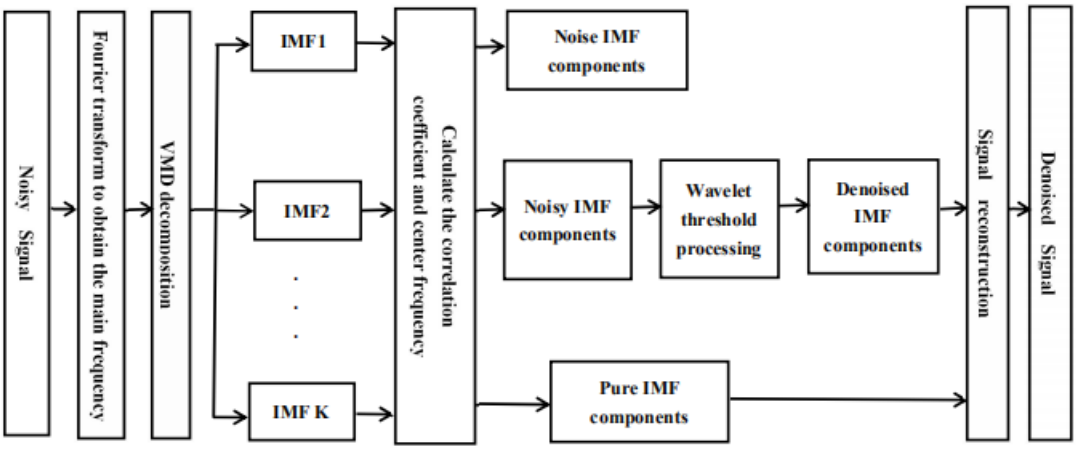

FIGURE 1. Flowchart of VMD-NWT method.

where the adjustment coefficient β is within the interval (0, 1), $\omega_{j,k}$ is the wavelet transform coefficients of the noisy observation signal, $sgn()$ is the symbolic function, thr is the threshold, and $\hat{w}_{j,k}$ is the estimated coefficients of the real signal. The estimated coefficients are between the soft and hard thresholds, but it is still discontinuous at the threshold points, thr and $-thr$. In addition, the denoising performance depend on the value of β .

An improved threshold function was proposed in [24], as shown in (9),

$$\hat{\omega}_{j,k} = \begin{cases} \omega_{j,k}, & |\omega_{j,k}| > thr \\ sgn(\omega_{j,k})\dfrac{2|\omega_{j,k}|}{thr}(|\omega_{j,k}| - \dfrac{thr}{2}), & \dfrac{thr}{2} \le |\omega_{j,k}| \le thr \\ 0, & |\omega_{j,k}| < \dfrac{thr}{2} \end{cases} \tag{9}$$

which overcomes the disadvantages of hard threshold discontinuity and the constant deviation between soft threshold estimated coefficients and real coefficients and thus retain some detailed information, but the threshold function is not properly adjusted according to the wavelet decomposition scale.

The wavelet threshold function used in NWT, as shown in (10), could retain detailed information as well as adaptively varying according to wavelet decomposition scale and has better denoising effect.

$$\hat{\omega}_{j,k} = \begin{cases} \omega_{j,k}, & |\omega_{j,k}| \ge thr \\ sgn(\omega_{j,k})\dfrac{|\omega_{j,k}|}{\dfrac{j}{j+1}thr}(|\omega_{j,k}| - \dfrac{j}{j+1}thr) \cdot (j+1), & \\ \qquad \dfrac{j}{j+1}thr \le |\omega_{j,k}| < thr & \\ 0, \quad |\omega_{j,k}| < \dfrac{j}{j+1}thr. & \end{cases} \tag{10}$$

where $\omega_{j,k}$ is the wavelet transform coefficients of the noisy observation signal, $sgn()$ is the symbolic function, thr is the threshold value, $\hat{\omega}_{j,k}$ is the estimated coefficients of the real signal, and j is the decomposition scale.

III. THE PROPOSED JOINT DENOISING METHOD BASED ON VMD AND NWT

VMD is a new method to adaptive non-recursive signal decomposition, which can decompose the noisy signal into an ensemble of relatively stable IMF components with less noise. Compared with EMD algorithms, VMD with strong mathematical theoretical basis and high computing rate can suppress high frequency noise and effectively reduce pseudo-component, mode mixing and endpoint effect et al. The wavelet′s frequency resolution is higher at low frequencies than that at high frequencies. Thus wavelet threshold processing method has better denoising effects on the analysis and processing of non-stationary signals and white noise signals and can preserve time-frequency characteristics of the signals at same time. If the two methods VMD and NWT are combined effectively, the denoising effect will be better than the single denoising method.

Based on the above analysis, a signal denoising method based on VMD and NWT is proposed in this paper, named by VMD-NWT. The flow chart of VMD-NWT method is shown in Fig.1 and the steps of VMD-NWT method are as follows:

Step 1: Obtain the main frequency f_0 of the noisy signal by Fourier transform and the IMF components by VMD.

Step 2: Calculate the correlation coefficients and center frequency f_k of each IMF component.

Step 3: Determine the noise IMF components, pure IMF components and noisy IMF components according to the correlation coefficient of each IMF component and $|f_k - f_0|$, the absolute value of the deviation between the center frequency f_k and the main frequency f_0 . The value of the correlation coefficients shows the correlation between IMF components and the signal. The more the noise contained in the components, the lower the correlation. In general, the correlation value of noise components is 0. We defined the IMF components with micro-correlation as noise IMF components,

and the real correlation components as noisy IMF components, The IMF components with the minimum $|f_k - f_0|$, i.e. its center frequency are closest to the main frequency reasonably, are taken as pure IMF components.

Step 4: Denoise the noisy IMF components as a whole by NWT processing, where using $db4$ wavelet and $3-$layer decomposition, discard the noise IMF components, and reserve the pure IMF components without any processing. Because the IMF components extracted from the noisy signals are relatively stable and has less noise, the NWT processing will has a better denoising effect on the certain components.

Step 5: Reconstruct the denoised noisy IMF components and pure IMF components to realize useful signal extraction.

IV. EXPERIMENTS

A. SIMULATION EXPERIMENTS

1) SIMULATION SIGNAL

In order to quantitatively evaluate the denoising performance of VMD-NWT, the known Gaussian white noise and baseline wander are added into the known clean sine signal to simulate the noisy signal received by the MEMS vector hydrophone. Thus the contaminated signal can be modeled as follows:

$$f(n) = s(n) + gs(n) + bs(n). \tag{11}$$

where $f(n)$ is the corrupted observed signal, $s(n)$ is the noise-free source signal, $gs(n)$ is the Gaussian white noise under different noise-added decibels, $bs(n)$ is the baseline drift noise, and n is the sampling point.

In this paper, the simulation source signal is a sequence of sine signal, defined as follows:

$$s(n) = 2 \cdot \sin(2\pi \cdot 400 \cdot n). \tag{12}$$

whose amplitude and frequency are 2 and $400Hz$, respectively.

And in this simulation experiment, $bs(n)$ is modeled by a superposition of a sine signal and a DC component as illustrated in (13),

$$s(n) = \sin(2\pi \cdot 50 \cdot n) + 1. \tag{13}$$

Due to the limited space, this paper uses the VMD-NWT method to process the noisy signal, whose Gaussian white noise level is at 4.8270 dB. Thus the noisy signal is obtained, shown in Fig. 2(a).

2) DENOISING THE SIMULATION SIGNAL BY VMD-NWT

Firstly Fourier transform on the noisy signal is carried out and its corresponding frequency spectrum is calculated, as shown in Fig.2(b), to obtain its main frequency f_0 . Then the noisy signal is decomposed into K IMF components by VMD. It should be noticed that the determination of the value of K and ε are two key factors which have important impact on the decomposition results. By decomposing the same signal using EMD method, K', the number of modes decomposed by the EMD method is obtained. A large number

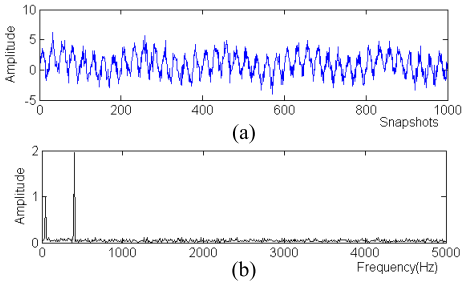

FIGURE 2. Noisy signal and its corresponding frequency spectrum. (a) Noisy signal. (b) Frequency spectrum of noisy signal.

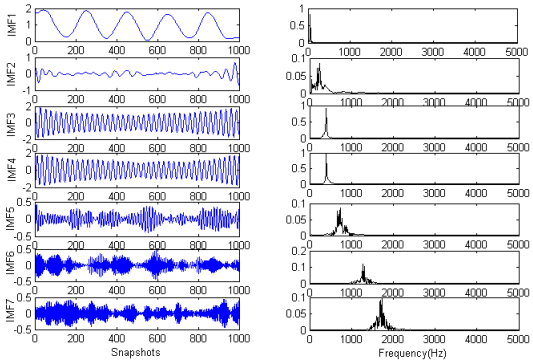

FIGURE 3. IMF components and corresponding frequency spectra.

of repeated denoising experiments using the VMD-NWT method are tested in which the K is set to K', $K' \pm 1$, $K' \pm 2$, respectively. And by analyzing the above denoising experimental results, K in the experiment of this paper is selected as 7. And ε is set as $1e-8$ to guarantee the decomposition accuracy. IMF components and their corresponding frequency spectra are shown in Fig.3. As can be seen from Fig.3, IMF3 and IMF4 have the highest energy, and their center frequencies are also around $400Hz$, which are closest to the main frequency f_0 . Thus, IMF3 and IMF4 are selected as the pure IMF components.

Then the correlation coefficient of each IMF component are calculated, shown in Table 1. The correlation coefficient of IMF7 is significantly lower than that of other IMF components and IMF7 has the second lowest energy in Fig.3. Therefore, IMF7 is considered to be the high-frequency noise component and then is discarded. IMF1, IMF2, IMF5 and IMF6 are considered to be the noisy IMF components and then they are denoised as a whole by NWT processing to obtain the denoised IMF components.

Finally the denoised IMF components and the pure IMF components reconstruct the denoised signals.

3) EXPERIMENTAL RESULTS

• comparison for denoised effects

In this paper, VMD-NWT, Complete Ensemble Empirical Mode Decomposition with Adaptive Noise combined with wavelet soft threshold processing method (CEEMDAN-WT),

TABLE 1. Correlation coefficient of each IMF component.

IMF component	$IMF1$	$IMF2$	$IMF3$	$IMF4$	$IMF5$	$IMF6$	$IMF7$
Correlation Coefficients	0.4127	0.2290	0.6276	0.6211	0.5937	0.1425	0.1081

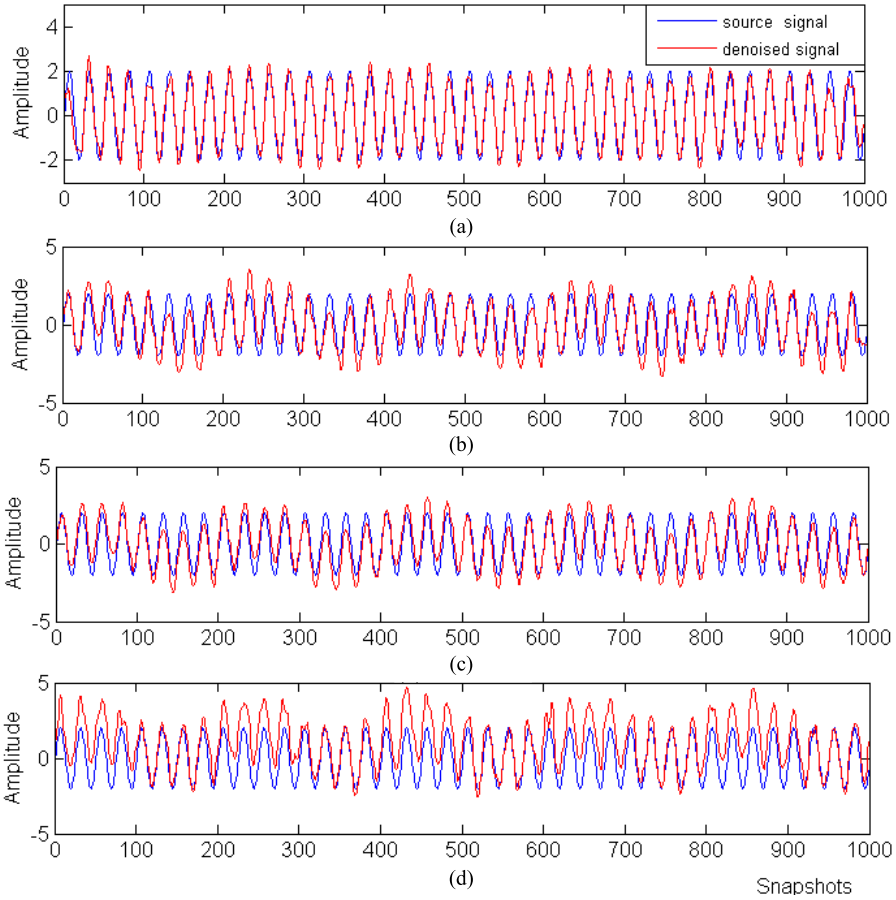

FIGURE 4. Denoised effects of four denoising methods: VMD-NWT, CEEMDAN-WT, EEMD-WT and ZWT. (a) VMD-NWT. (b) EEMD-WT. (c) ZWT.

Ensemble Empirical Mode Decomposition combined with wavelet soft threshold processing method (EEMD-WT), and single wavelet threshold processing method with compromised function between hard and soft threshold (ZWT) are employed to denoise the same noisy signal for comparison, and the denoised effects comparison of VMD-NWT, CEEMDAN-WT, EEMD-WT and ZWT between the source signal and the denosied signal are shown in Fig.4.

From Fig.4(a), the denoised signal obtained by VMD-NWT can fit the source signal well, where the sharp burrs have been effectively eliminated and the whole becomes smooth and neat, with little distortion phenomenon. And the baseline of the denoised signal is almost completely coincident with that of the source signal, which performs the correction of baseline drift well.

The denoised performances of CEEMDAN-WT, EEMD-WT and ZWT are shown in Fig.4 (b), Fig.4 (c) and Fig.4(d), respectively. Though the most white noises of the signal are well eliminated, there are local distortion phenomenons at the signal extreme points which made the further signal detection and recognition in trouble. In Fig.4(b) and Fig.4(c), both the DC component baseline of the denoised signal have been corrected to the zero level, but the overall sine drift phenomenon have not been corrected and there are still significant fluctuations. In Fig.4(d), the phenomenon of baseline drift is hardly corrected and there are still the phenomenon of sine and DC wander. Based on the above analyses, the conclusion is drawn that in this experiment, the denoised effect of VMD-NWT is better than that of CEEMDAN-WT, EEMD-WT and ZWT.

• comparison for denoised performance indicators

In order to further verify the effectiveness and advantages of VMD-NWT, the denoised performance indicators are introduced, Signal-to-Noise Ratio (SNR),

$$SNR = 10\log(\frac{\sum_n x^2(n)}{\sum_n [x(n) - \hat{x}(n)]^2}). \tag{14}$$

TABLE 2. Comparison of denoising performance indicators of each method.

Gaussian White Noise	SNR_{in}	Performance indicator	VMD-NWT	CEEMDAN-WT	EEMD-WT	ZWT
9.8524	4.3830	SNR	16.4701	5.8015	5.7492	5.7524
		$RMSE$	0.2063	0.7252	0.7295	1.2410
4.8270	2.4186	SNR	15.5773	5.0898	5.1459	4.3741
		$RMSE$	0.2353	0.7873	0.7820	1.2967
-0.5006	-1.3912	SNR	11.2458	3.7665	3.6402	3.3338
		$RMSE$	0.3875	0.9166	0.9301	1.3823
-4.8572	-5.6965	SNR	11.1812	0.3121	0.8410	0.3487
		$RMSE$	0.3904	0.3643	1.2838	1.6568
-10.0722	-10.4997	SNR	6.5766	-3.1049	-3.1209	-4.5743
		$RMSE$	0.6633	2.0221	2.0257	2.5647

and Root Mean Square Error (*RMSE*),

$$RMSE = \sqrt{\frac{\sum_n [x(n) - \hat{x}(n)]^2}{N}}. \tag{15}$$

where n denotes the number of sampling points, N denotes the length of the signal, $x(n)$ denotes the source signal and $\hat{x}(n)$ denotes the denoised signal. What we can see from (14) and (15) is that the samller the value of $\sum_n [x(n) - \hat{x}(n)]^2$ is, namely the smaller the sum of the squares of the deviation between the observed value and true value is, the higher the *SNR* is, and the lower the *RMSE* is. So the higher *SNR* and the lower *RMSE* of the output signal means the smaller deviation between the observed value and true value, which means the better denoised effect.

The noisy signals with five different decibel noise are used to be denoised by the above four methods: VMD-NWT, CEEMDAN-WT, EEMD-WT and ZWT, respectively. The denoised performance indicators are shown in Table 2.

In Table 2, the first column represents the *SNR* value of signal with only Gaussian white noise, and the second column SNR_{in} represents the *SNR* value of the observed signal with both Gaussian white noise and baseline drift noise.

We have known that the higher the *SNR* and the lower the *RMSE* of the output signal, the better the denoised effect. From Table 2, it can be seen that the denoised effect of VMD-NWT is significantly better than those of the other three methods CEEMDAN-WT, EEMD-WT and ZWT under different decibel noises. The denoising effect of CEEMDAN-WT and EEMD-WT is similar, and both effects are slightly better than that of ZWT. All of these further demonstrate that the proposed method VMD-NWT has a better denoised effect on noisy signal with different decibel noise and baseline drift, which proves the effectiveness and practicability of the proposed method VMD-NWT in this paper.

B. LAKE TRIAL EXPERIMENTS

According to the principle of bionics, the MEMS vector hydrophone realizes the underwater sound signal detection through detecting the change of resistance. The MEMS vector hydrophone has passed the test and has the advantages of high sensitivity, wide frequency response range and good "8" shape cosine directivity [1], et al.

The measured data used in this paper are derived from fenji experiments conducted by North university of China in 2011 and 2014 in fenhe, respectively.

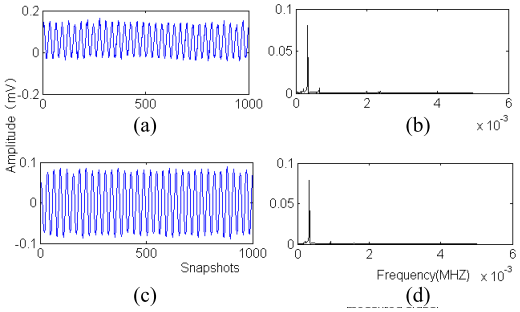

FIGURE 5. X road signal of 1♯ hydrophone (2011.10). (a) Noisy measured signal. (b) Frequency spectrum of noisy measured signal. (c) Denoised measured signal. (d) Frequency spectrutn of denoised measured signal.

1) EXPERIMENTS 1: THE MEASURED DATA ARE SELECTED FROM THE FENJI331HZ DATA PACKET TESTED IN OCTOBER 2011.

In the experiment, the hydrophone array (MEMS vector hydrophone with 4-element linear array and spacing 1 meter) was fixed on the shore, and the transducer was placed on the tugboat. With the distance between the arrays and the tugboat gradually increasing, different positions are selected to drop anchor and obtain the collected data by using the transducers. And the sound source with a transmitting signal frequency of $331Hz$ is 6 meters away from the vector hydrophone with a sampling frequency of $10kHz$. The experimental data with a length of 1000 snapshots are randomly intercepted from the X and Y road original collected data of 1♯ and 2♯ hydrophone, respectively.

Fig.5-Fig.8 show the signals of the experimental data and corresponding frequency spectra, as well as the denoised signal and their frequency spectra processed by VMD-NWT.

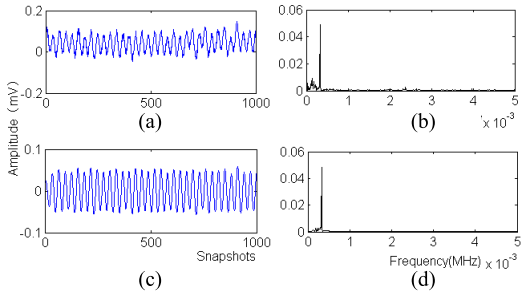

FIGURE 6. Y road signal of 1♯ hydrophone (2011.10). (a) Noisy measured signal. (b) Frequency spectrum of noisy measured signal. (c) Denoised measured signal. (d) Frequency spectrum of denoised measured signal.

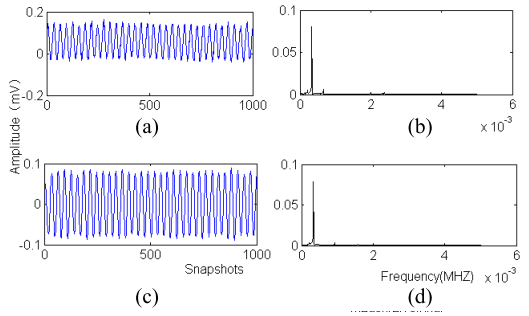

FIGURE 7. X road signal of 2♯ hydrophone(2011.10). (a) Noisy measured signal. (b) Frequency spectrum of noisy measured signal. (c) Denoised measured signal. (d) Frequency spectrum of denoised measured signal.

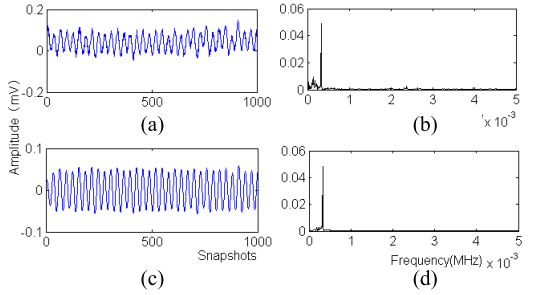

FIGURE 8. Y road signal of 2♯ hydrophone(2011.10). (a) Noisy measured signal. (b) Frequency spectrum of noisy measured signal. (c) Denoised measured signal. (d) Frequency spectruln of denoised theasured signal.

It can be observed from the subgraph (*a*) and (*b*) of Fig.5-Fig.8 that the X road and Y road signal of 1♯ hydrophone and the X road signal of 2♯ hydrophone contain a small amount of noise and the Y road signal of 2♯ hydrophone contains a large amount of noise. The four road of signal all have relatively slow varying baseline drift phenomenons, and the baselines have deviated from the zero level and exist overall fluctuation. Subgraph (*c*) and (*d*) of Fig.5-Fig.8 are the denoised signals and their frequency spectra of the four-road measured signal using the VMD-NWT. On the one hand, in the Subgraph (*c*) of Fig.5-Fig.8, the sharp burrs of the signals have been effectively eliminated, the distorted part of the signal is effectively corrected, and the signal become smooth and tidy. Moreover, in the

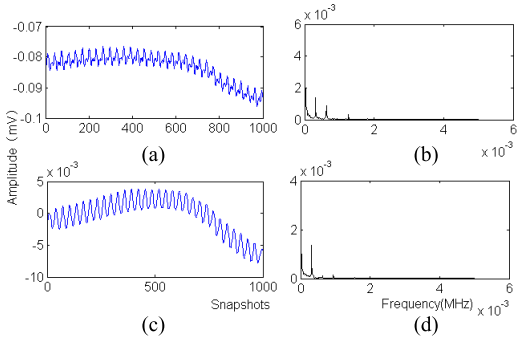

FIGURE 9. X road signal with 315*Hz* of 2♯ hydrophone(2014.9). (a) Noisy measured signal. (b) Frequency spectrum of noisy measured signal. (c) Denoised measured signal. (d) Frequency spectrun of denoised measured signal.

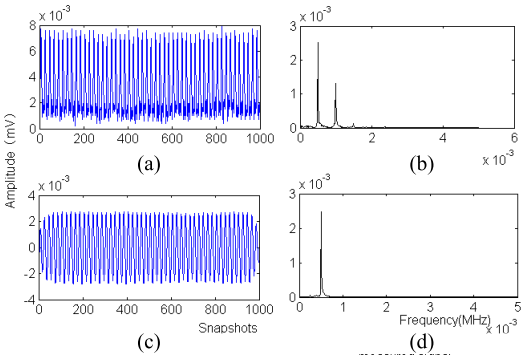

FIGURE 10. X road signal with 500*Hz* of 2♯ hydrophone(2014.9). (a) Noisy theasured signal. (b) Frequency spectrum of noisy measured signal. (c) Denoised measured signal. (d) Frequency spectrum of denoised measured signal.

Subgraph (*d*) of Fig.5-Fig.8, the energy of the signals are hardly no loss. On the other hand, the drifted baselines are all well corrected and the signal baselines have been corrected to the zero level.

2) EXPERIMENTS 2: THE MEASURED DATA ARE SELECTED FROM THE FENJI MEASURED DATA IN SEPTEMBER 2014

The MEMS vector hydrophone arrays with 5-element array and spacing 0.5 meter are fixed on the shore and the transducers are placed on a tugboat. The hydrophone was placed 2 meters below the water, and the arrays were kept in a horizontal state, which made the hydrophone continuously output sound pressure and circuit signal. The transducer was adjusted to transmit single-frequency signals with 315*Hz*, 500*Hz*, 630*Hz*, 800*Hz* and 1000*Hz* respectively.

In this section, the experimental data also with a length of 1000 snapshots are randomly intercepted from original collected data with 315*Hz*, 500*Hz*, 630*Hz*, 800*Hz* and 1000*Hz* of X road of 2♯ hydrophone, respectively. Fig.9 - Fig.13 show the original measured signal with 315*Hz*, 500*Hz*, 630*Hz*, 800*Hz* and 1000*Hz* and their corresponding frequency spectra, as well as the denoised signal processed by the VMD-NWT and their corresponding

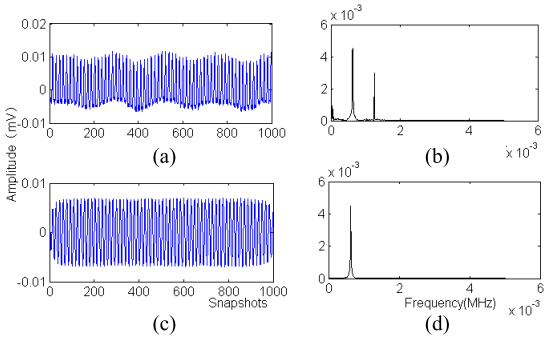

FIGURE 11. X road signal with 630*Hz* of 2♯ hydrophone(2014.9). (a) Noisy measured signal. (b) Frequency spectrum of noisy measured signal. (c) Denoised measured signal. (d) Frequency spectrum of denoised measured signal.

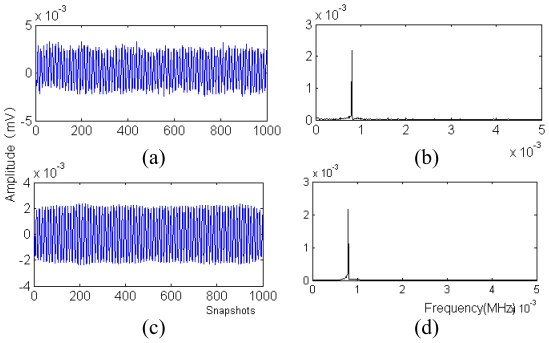

FIGURE 12. X road signal with 800*Hz* of 2♯ hydrophone(2014.9). (a) Noisy measured signal. (b) Frequency spectrum of noisy measured signal. (c) Denoised measured signal. (d) Frequency spectrun of denoised theasured signal.

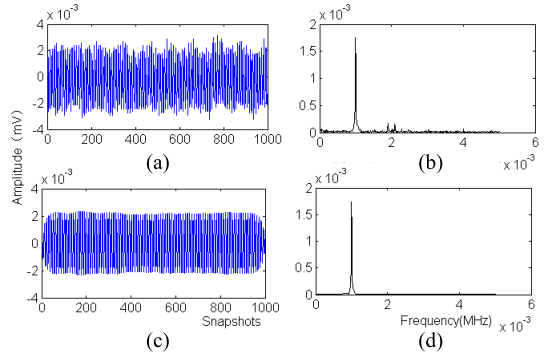

FIGURE 13. X road signal with 1000*Hz* of 2♯ hydrophone(2014.9). (a) Noisy measured signal. (b) Frequency spectrum of noisy measured signal. (c) Denoised measured signal. (d) Frequency spectrum of denoised measured signal.

frequency spectra, respectively. It can be observed that, in Fig.9(a) and (b), signal distortion is severe and there is a large drift in signal baseline; in Fig.10(a) and (b), there are high frequency noise in the lower half of the signal, causing significant distortion on the signal waveform and the signal baseline deviates the zero level, namely a slightly drift; in Fig.11(a) and (b), there are low frequency noise in upper part of the signal and high frequency noise in the lower part so that the signal has been seriously distorted and the baseline is deviates the zero level and has a obvious drift; in Fig.12(a) and (b), little noise exist in the signal and the baseline slightly deviates the zero level but have obvious drift phenomenon; in Fig.13(a) and (b), just little noise exist in the signal and the baseline drift phenomenon is not obvious. After the measured signal were denoised by VMD-NWT, in Fig.9(c), the noise is well eliminated and the waveform has been better recovered. But due to the large fluctuation in original measurement data, may be caused by sudden noises arrivals of external environment, such as arrivals of ships and storms, or the hardware equipment failures, the volatility of denoised signal is also relatively large and need a further processing. The noise in the measured signal of 500*Hz*, 630*Hz*, 800*Hz* and 1000*Hz* have been effectively eliminated, the basic characteristics of the original signal are well retained and with less distortion in the signal, and the drift baseline have been effectively corrected to the zero level in Fig.10(c) - Fig.13(c). At the same time, from the comparison between Subfigure (b) and (d) of Fig.9 - Fig.13, the energy of the denoised measured signal have been preserved with no loss.

3) EXPERIMENTAL RESULTS

It can be concluded from the above two trial experiments that the proposed VMD-NWT method in this paper can effectively eliminate the noise of the vast majority of measured signal, recover the basic characteristics of the source signal better and make the baseline drift well corrected. Thus the VMD-NWT method could lay a good foundation for the further MEMS hydrophone signal detection and recognition.

V. CONCLUSION

In this paper, a signal denoised method (VMD-NWT) based on VMD and NWT processing is proposed to the problem of strong noise interference and baseline drift in the data acquisition of MEMS vector hydrophone. The VMD-NWT method has simple principle and less calculation, which can effectively remove the noise of the signal and correct the phenomenons of baseline drift. The VMD-NWT method is compared with CEEMDAN-WT, EEMD-WT and ZWT methods by a large number of repeating simulation experiments. The results show that the VMD-NWT method is superior to the CEEMDAN-WT, EEMD-WT and ZWT methods both on the intuitive denoised effect and the quantitative denoised performance indicators. In lake trial experiments, the noises of the measured data are effectively eliminated by VMD-NWT. And the basic characteristics of the signal are well preserved with almost no energy loss. And the phenomenons of baseline drift are also corrected to zero level well. Therefore, it is concluded that the VMD-NWT method proposed in this paper has certain practical research value and can lay a good foundation for the further MEMS hydrophone signal detection and identification. Our future research work is hope to realize adaptive denoising procedure by using

suitable intelligent optimization algorithm to adaptively find the best VMD parameters.

REFERENCES

[1] C. Xue, S. Chen, W. Zhang, B. Zhang, G. Zhang, and H. Qiao, "Design, fabrication, and preliminary characterization of a novel MEMS bionic vector hydrophone," *Microelectron. J.*, vol. 38, nos. 10–11, pp. 1021–1026, Oct./Nov. 2007.
[2] G.-J. Hang, Z. Li, S.-J. Wu, C.-Y. Xue, S.-E. Yang, and W.-D. Zhang, "A bionic fish cilia median-low frequency three-dimensional piezoresistive MEMS vector hydrophone," *Nano-Micro Lett.*, vol. 6, no. 2, pp. 136–142, Apr. 2014.
[3] P. Wang, "Research on the DOA estimation and localization technology to acoustic target for MEMS vector hydrophone array," Ph.D. dissertation, North Univ. China, Taiyuan, China, 2013.
[4] V. V. Baskar, V. Rajendran, and E. Logashanmugam, "Study of different denoising methods for underwater acoustic signal," *J. Mar. Sci. Technol.*, vol. 23, no. 4, pp. 414–419, 2015.
[5] S. Luo and P. Johnston, "A review of electrocardiogram filtering," *J. Electrocardiol.*, vol. 43, no. 6, pp. 486–496, Nov./Dec. 2010.
[6] R. P. Narwaria, S. Verma, and P. K. Singhal, "Removal of baseline wander and power line interference from ECG signal—A survey approach," *Int. J. Electron. Eng.*, vol. 3, no. 1, pp. 107–111, 2011.
[7] P. Laguna, R. Jané, E. Masgrau, P. Caminal, "The adaptive linear combiner with a periodic-impulse reference input as a linear comb filter," *Signal Process.*, vol. 48, no. 3, pp. 193–203, Feb. 1996.
[8] D. Wei and Y. M. Li, "Generalized wavelet transform based on the convolution operator in the linear canonical transform domain," *Opt.-Int. J. Light Electron Opt.*, vol. 125, no. 16, pp. 4491–4496, Aug. 2014.
[9] D. B. Percival and A. T. Walden, *Wavelet Methods for Time Series Analysis*. Cambridge, U.K.: Cambridge Univ. Press, 2000.
[10] G. Han and Z. Xu, "Electrocardiogram signal denoising based on a new improved wavelet thresholding," *Rev. Sci. Instrum.*, vol. 87, no. 8, Aug. 2016, Art. no. 084303.
[11] L. Xu, D. Zhang, K. Wang, N. Li, and X. Wang, "Baseline wander correction in pulse waveforms using wavelet-based cascaded adaptive filter," *Comput. Biol. Med.*, vol. 37, no. 5, pp. 716–731, May 2007.
[12] N. E. Huang *et al.*, "The Empirical Mode Decomposition and Hilbert spectrum for nonlinear and non-stationary time series analysis," *Proc. Roy. Soc. London Ser. A, Math., Phys. Eng. Sci.*, vol. 454, no. 1, pp. 903–995, Mar. 1998.
[13] T. Wang, M. Zhang, Q. Yu, and H. Zhang, "Comparing the applications of EMD and EEMD on time–frequency analysis of seismic signal," *J. Appl. Geophys.*, vol. 83, pp. 29–34, Aug. 2012.
[14] K.-M. Chang and S.-H. Liu, "Gaussian noise filtering from ECG by Wiener filter and ensemble empirical mode decomposition," *J. Signal Process. Syst.*, vol. 64, no. 2, pp. 249–264, Aug. 2011.
[15] Z. D. Zhao, J. Liu, and S. Wang, "Denoising ECG signal based on ensemble empirical mode decomposition," *Proc. SPIE-Int. Soc. Opt. Eng.*, vol. 8285, no. 23, Oct. 2011, Art. no. 828577.
[16] N. Mariyappa *et al.*, "Baseline drift removal and denoising of MCG data using EEMD: Role of noise amplitude and the thresholding effect," *Med. Eng. Phys.*, vol. 36, no. 10, pp. 1266–1276, Oct. 2014.
[17] K. Dragomiretskiy, and D. Zosso, "Variational mode decomposition," *IEEE Trans. Signal Process.*, vol. 62, no. 3, pp. 531–544, Feb. 2014.
[18] Z. Wang *et al.* "Application of parameter optimized variational mode decomposition method in fault diagnosis of gearbox," *IEEE Access*, vol. 7, pp. 44871–44882, Apr. 2019.
[19] Y. Li, G. Cheng, C. Liu, and X. Chen, "Study on planetary gear fault diagnosis based on variational mode decomposition and deep neural networks," *Measurement*, vol. 130, pp. 94–104, Dec. 2018.
[20] S. Lahmiri, "Intraday stock price forecasting based on variational mode decomposition," *J. Comput. Sci.*, vol. 12, pp. 23–27, Jan. 2016.
[21] L. Wen, Z. S. Liu, and Y. J. Ge, "Several methods of wavelet denoising," *J. Hefei Univ. Technol., Natural Sci.*, vol. 25, no. 2, p. 2, Apr. 2002.
[22] D. L. Donoho and I. M. Johnstone, "Ideal spatial adaptation by wavelet shrinkage," *Biometrika*, vol. 81, no. 3, pp. 425–455, Sep. 1994.
[23] R. Z. Zhao, G. X. Song, and H. Wang, "Better threshold estimation of wavelet coefficients for improving denoising," *J. Northwestern Polytech. Univ.*, vol. 19, no. 4, pp. 625–628, Jan. 2001.
[24] W. W. Jiang *et al.*, "Research on spectrum signal denoising based on improved threshold with lifting wavelet," *J. Electron. Meas. Instrum.*, vol. 28, no. 12, pp. 1363–1368, Dec. 2014.

HONGPING HU received the Ph.D. degree from the North University of China, Shanxi, China, in 2009, where she is currently an Associate Professor and a master's tutor with the Department of Mathematics. Her research interests include combinatorial mathematics, artificial intelligence, and image processing.

LINMEI ZHANG received the bachelor's degree from the Department of Mathematics, Taiyuan Normal University of China, Shanxi, China, in 2017. She is currently pursuing the M.S. degree with the School of Science, North University of China. Her current research interests include artificial intelligence, signal processing, and intelligent optimization algorithm.

HUICHAO YAN is currently pursuing the Ph.D. degree with the School of Information and Communication Engineering, North University of China. His current research interests include artificial intelligence, signal processing, and intelligent optimization algorithm.

YANPING BAI received the Ph.D. degree from the North University of China, Shanxi, China, in 2005, where she is currently a Professor and a Ph.D. Tutor with the School of Information and Communication Engineer. Her research interests include optimization algorithm, artificial intelligence, signal processing, image processing, and MEMS reliability research.

PENG WANG received the Ph.D. degree from the North University of China, Shanxi, China, in 2013, where he is currently an Associate Professor and a master's tutor with the Department of Mathematics. His research interests include combinatorial mathematics, artificial intelligence, and signal processing.